

Simulating soil water regime in lowland paddy fields under different water managements using HYDRUS-1D

Xuezhi Tan ^{a,b}, Dongguo Shao ^{a,*}, Huanhuan Liu ^a

^a State Key Laboratory of Water Resources and Hydropower Engineering Science, Wuhan University, Wuhan 430072, PR China

^b Department of Civil and Environmental Engineering, University of Alberta, Edmonton, Alberta, Canada T6G 2W2



ARTICLE INFO

Article history:

Received 27 April 2013

Accepted 13 October 2013

Available online 5 November 2013

Keywords:

Paddy soil

Soil water flow

Soil water pressure

Alternate wetting and drying (AWD)

Groundwater capillary rise

HYDRUS-1D

ABSTRACT

The widely adopted alternate wetting and drying (AWD) irrigation for rice production in lowland paddy fields with shallow groundwater table is increasingly needed to quantify the soil water regime for irrigation schedule design. Field experiments were conducted to compare the soil water flow between paddy fields under AWD and continuously flooded irrigation (CFI), during the rice growing season in 2010–2011. Model simulations using HYDRUS-1D were also conducted based on the measured pressure head distribution of soil profiles. Modeling results show that the pressure head derived from forward simulation using the point estimated soil hydraulic parameters did not agree well with the measured pressure head. However, from inverse modeling of saturated hydraulic conductivities of plow pan (mean of 0.68 cm d^{-1} in AWD plots and 0.54 cm d^{-1} in CFI plots), the HYDRUS-1D model can properly simulate the water flow in multi-layer paddy soil flow, where the plow pan plays an important role in determining the vertical pressure head distribution. The measured pressure head and simulated pressure head derived from inverse modeling agreed well (NSE of 0.93–0.98) during the whole rice growing season. Measurement and simulation results indicated that the practice of AWD decreased the percolation 38.2–40.3% in 2010 and 23.3–27.2% in 2011, compared to that of CFI. It is also found that groundwater capillary rise amounted to 26.1–27.4% in AWD plots, and 10.2–18.1% in CFI plots of respective water input (irrigation and rainfall).

© 2013 Elsevier B.V. All rights reserved.

1. Introduction

Rice is a large water consumer, but water for rice production is increasingly becoming scarce and expensive due to the increasing demand for water from the ever-growing population, competition for water from other sectors, such as urbanization, tourism, industry and ecosystem services (Bouman and Tuong, 2001; Loeve et al., 2007). Water-saving irrigation (WSI) methods, e.g. alternate wetting and drying (AWD), saturated soil culture, aerobic rice, have been widely adopted for rice production in Asia, where rice accounts for 40–46% of the net irrigated area of all crops (Li and Barker, 2004; Bouman et al., 2007b). The WSI methods do not require rice fields to be continuously flooded. Farmers only irrigate and re-flood their fields when field soil moisture or soil matric potential is lower than the threshold value, below which rice yield will decrease significantly.

Many reported studies suggested that WSI methods do not reduce the rice yield, and sometimes it may improve rice root and shoot growth, and enhance rice yield (Bouman et al., 2007b;

Cabangon et al., 2004; Zhang et al., 2009). The success of WSI implementation for reducing water input (rainfall and irrigation) is mostly due to the decrease of water losses through seepage and percolation, since the hydrostatic pressure can be significantly reduced compared to continuously flooded irrigation (CFI) field (Kukal et al., 2005). Some research has been done to quantitatively assess different water outflows, i.e., evaporation, seepage and percolation in lowland AWD paddy fields, but the water balance analysis of AWD fields was usually assumed that there was no groundwater capillary rise (also referred as upward water flux or groundwater inflow) in fields under AWD (Luo et al., 2009). The reduction of seepage and percolation benefiting from AWD practice was overestimated (Cabangon et al., 2004; Bouman et al., 2007b; Peng et al., 2011). The groundwater capillary rise is difficult to be measured and simulated by simple soil water movement models, e.g. ORYZA2000 with SAWAH (ten Berge et al., 1995; Bouman et al., 2001; Belder et al., 2007), although it has been used to simulate the effects of groundwater depth on yield-increasing interventions (Boling et al., 2007). Admittedly, the infiltration of paddy fields also affects the groundwater recharge and groundwater table fluctuation (Mishra et al., 1990; Liu et al., 2005). The impacts of AWD on groundwater capillary rise and rice yields were not well understood to improve AWD practice.

* Corresponding author. Tel.: +86 13986298750.

E-mail address: dgshao@whu.edu.cn (D. Shao).

Under AWD practice, the soil water regime of paddy fields is transformed from being saturated to being alternately saturated and unsaturated. Thus, the soil water movement between paddy fields under AWD and under CFI differs greatly. To reduce water use without affecting rice yield by AWD, groundwater depth are usually required to be extremely shallow (Belder, 2004; Bouman et al., 2007b). Tuong et al. (2005) suggested that irrigation should be based on a threshold soil matric potential at 10 cm depth of -20 kPa, while Kukal et al. (2005) reported that irrigation should be conducted when the soil matric potential at 15–20 cm depth is lower than -16 kPa. Luo et al. (2009) even suggested that the irrigation scheduling criteria can be set as -30 kPa for average root zone soil matric potential, whereas it can be set at -70 kPa during the dry years for aerobic rice. These critical soil matric potentials are all derived from specific field experiments with different soil physical properties. The relationship between groundwater depth and critical soil matric potential was not fully demonstrated for field water management. With an irrigation criterion of soil matric potential, the total amount of irrigation water input was a function of the number of rainy days and evaporation during the rice season (Kukal et al., 2005). From the simulation results of Boling et al. (2007), the rice yields in fields under AWD, where groundwater depth is deeper than 0.5 m, may be lower than the potential yields. However, many paddy fields, where the groundwater depth reach 60 cm or more, and have reliable and timely irrigation water sources, also adopted AWD successfully without affecting rice yields (Peng et al., 2011). This may be due to the specific soil hydraulic properties and timely irrigation. It is needed to determine the critical soil matric potential based on groundwater depth and field soil properties.

Modeling of soil water movement is a possible way to assess the groundwater contribution to decrease irrigation water input in paddy fields under AWD. Because the saturated hydraulic conductivity of plow pan is extremely lower than that of its upper and lower soils, plow pan determines the vertical water movement and soil matric potential distribution in paddy fields (Wopereis et al., 1994; Chen and Liu, 2002). Conceptual models were popularly used for water balances assessment for AWD paddy fields, although it usually ignored groundwater capillary rise (Bouman et al., 2007a; Inthavong et al., 2011; Khepar et al., 2000). Luo et al. (2009) applied system dynamics approach to simulate time varying water balance in AWD paddy fields considering the groundwater capillary rise. Mechanical models, e.g. SAWAH (ten Berge et al., 1995) and FEMWATER (Chen et al., 2002), HYDRUS (Garg et al., 2009; Janssen and Lennartz, 2009) have been preliminarily applied to analyze the multi-layer soil water flow in paddy fields. However, the water balance of paddy fields under different water management was seldom examined using numerical models and taking groundwater capillary rise into consideration.

Thus, the objective of this study is to measure the pressure head distribution in the layered lowland paddy fields under AWD and CFI, and to model water flow for water balance analysis. The HYDRUS-1D model was used for simulating the soil water flow based on measured soil hydraulic parameters and pressure data.

2. Materials and methods

2.1. Field experiments

Field experiments on rice (*Oryza sativa*) were conducted for two years (2010–2011) during the rice growing season, at an experimental lowland paddy field ($112^{\circ}10'$, $30^{\circ}49'$; elevation of 72 m) of Zhanghe Irrigation District, which is located in Tuanlin, Hubei province and has been intensively researched on the

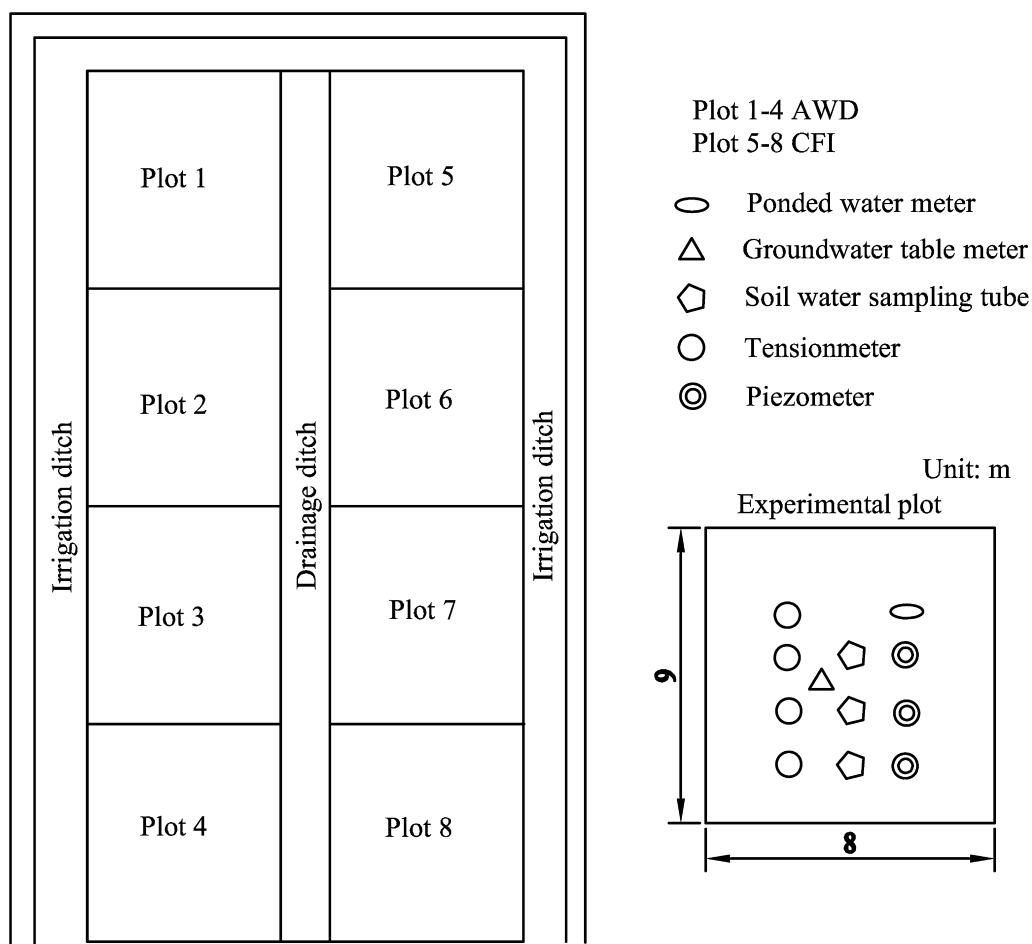
performance of water-saving irrigations in paddy fields (Belder, 2004; Cabangon et al., 2004). Two water treatments (AWD and CFI), with four replications were laid out in a split-plot design (Fig. 1). The concrete block levees divided the experimental plots (9 m \times 8 m) and they were covered with galvanized plastic plain sheet extending downward about 50 cm deep to minimize seepage across plots.

The controlled thresholds of field water regime in different rice growth stages for AWD irrigation are shown in Table 1, while paddy plots under CFI were maintained ponded water during the rice growing season, except in the growth stage of late tillering and yellow ripening when rice needs little water. In CFI paddy fields, irrigation was conducted immediately when there was no ponded water in fields. The upper limit depth of ponded water for both CFI and AWD paddy plots was 10 cm. At the rice growth stage of late tillering and yellow ripening, all paddy plots were drained for increasing rice yields as local farmers did (Mao, 2001; Li, 2001). Previous experiments proved that this AWD irrigation schedule can maintain and sometimes increase the rice yields (Tan et al., 2013). The same nitrogen and phosphorus fertilization was applied during the experiments.

Soil profile of each experimental paddy plot was excavated for soil cores sampling. Based on the in situ soil texture visual observation, as well as the soil property analysis, we divided up the soil profile into three layers, i.e., cultivated horizon layer (CHL), plow pan layer (PPL) and illuvial horizon layer (IHL) (Table 2). Disturbed soil used for texture analysis was sampled at each layer for each plot. The particle size distribution was determined by the soil particle size and shape measurement system (AZ-S0300) from the Ankersmid Ltd., Eytetech Series. At every layer of each plot, three replicates of 250 cm^3 soil cores were horizontally evenly sampled. These undisturbed soil cores samples were separated to three groups for analysis of bulk density, saturated hydraulic conductivity and water retention characteristics, respectively. Bulk density was determined with the familiar stove-drying method, and saturated hydraulic conductivity was measured with the constant head method. Soil water retention was determined with the Hyprop System based on the simplified evaporation method (Peters and Durner, 2008). With the measured core soil water potential and soil water content, the Hyprop System optimized van Genuchten's θ - h relationships which were used for HYDRUS-1D simulation and will be described in the next section.

Before rice transplanting, piezometers and tensiometers were installed in the center of each plot at soil depth of 18 and 33 cm where the pressure gradients were very large, as well as soil depth of 72 cm which was the deepest location that our tensiometers could reach. In order to measure the depth of groundwater table, each plot was drilled and embedded with PVC tube (4 cm in inner diameter) to form groundwater table meter. Paddy ponded water meters were also set up in each plot. The ponded water depths were able to be controlled through gates constructed at plots drainage outlets.

During the rice growing season in 2010 (June 3–September 25) and 2011 (June 9–September 28), the daily ponded water depth and water table of each paddy plot was measured by water level indicators and recorded manually. The daily soil pressure head measured by tensiometers was recorded. If the soil was saturated, the soil pressure head was measured by piezometers and recorded manually. All these daily value were read at 2:00 pm to ensure the consistency of data. The water components measured includes rainfall, irrigation, and drainage. Irrigation was conducted according to measured field water pressure head and irrigation schedule. The amount of irrigation volume was 30 mm a time as local farmers did, by controlling the pumping time with steady pumping flow. It should be noted that there was no drainage water observed at the outlets of both AWD and CFI paddy plots. The

**Fig. 1.** Schematic of the field layout and locations of instruments.**Table 1**

Controlled thresholds of field water regime in different rice growth stages for AWD irrigation.

Irrigation	TG	ET	LT	BH	MR	YR
Upper ponded water depth limited (cm)	10	10	10	10	10	
Lower pressure head limited (cm) ^a	0	-50	-150	-100	-50	
Observed depth (cm)	18	18	18	33	33	Drainage and naturally drying

TG, turning green; ET, early tillering; LT, late tillering; BH, booting and heading; MR, milk ripening; YR, yellow ripening.

^a Data show the pressure head at the observed depth where tensiometers located.

daily evapotranspiration was calculated by multiplying reference evapotranspiration, derived from Penman–Monteith Equation, by the rice coefficient (Allen et al., 1998). The meteorological data were obtained from the Tuanlin Weather Station that is 100 m away from the experimental paddy plots. The seasonal grain yields at the harvest time were investigated in each year for all plots. In this paper, dates used in rice growing season were referred to as days after transplanting (DAT).

2.2. Model simulation

Water flow was modeled using the HYDRUS-1D (Simunek et al., 1998), in which water flow is described by the Richards equation:

$$\frac{\partial \theta}{\partial t} = \frac{\partial}{\partial Z} \left[K(h) \left(\frac{\partial h}{\partial Z} + 1 \right) \right] - S \quad (1)$$

Table 2

Basic physical properties of soils from paddy plots by core sample laboratory analysis.

Soil layer	Texture			ρ_b (g cm^{-3})	Parameters of the water retention equation			K_s (cm d^{-1})
	Sand (%)	Silt (%)	Clay (%)		θ_r ($\text{cm}^{-3} \text{cm}^{-3}$)	θ_s ($\text{cm}^{-3} \text{cm}^{-3}$)	α (cm^{-1})	
Cultivated horizon layer (CHL) (0–18 cm)	20.2	45.5	34.3	1.33 (6.43) ^a	0.098 (42)	0.43 (32)	0.021 (12)	1.31 (10) 7.43 (32)
Plow pan layer (PPL) (18–33 cm)	16.1	44.7	39.2	1.56 (2.58)	0.069 (53)	0.38 (28)	0.011 (14)	1.23 (11) 0.48 (46)
Illuvial horizon layer (IHL) (33–100 cm)	36.4	37.2	26.4	1.43 (2.79)	0.062 (31)	0.41 (25)	0.034 (8)	1.41 (8) 18.2 (11)

ρ_b , bulk density; θ_r , residual volumetric water contents; θ_s , saturated volumetric water contents; α and n , fitting parameters of soil water characteristic curve; K_s , saturated hydraulic conductivity.

^a Values in the parenthesis indicate the coefficients of variation (CV) expressed in percentage.

where t is the time (d), θ is the volumetric water content ($\text{cm}^3 \text{cm}^{-3}$), h is the soil water pressure head (cm), Z is the spatial coordinate (cm) defined as positive upward, $K(h)$ is the unsaturated hydraulic conductivity function (cm d^{-1}) and S is a sink term representing water uptake by plant roots (cm d^{-1}), which is the daily evapotranspiration.

We used van Genuchten's $K-h$ and $\theta-h$ relationships for describing soil hydraulic properties of lowland paddy soils (van Genuchten, 1980):

$$\theta(h) = \theta_r + \frac{\theta_s - \theta_r}{[1 + (\alpha h)^n]^m}, \quad h \leq 0 \quad (2)$$

$$K(h) = K_s S_e^l (1 - (1 - S_e^{1/m})^m)^2 \quad (3)$$

with $m = 1 - \frac{1}{n}$ and $S_e = \frac{\theta - \theta_r}{\theta_s - \theta_r}$

where θ_r and θ_s denote the residual and saturated volumetric water contents ($\text{cm}^3 \text{cm}^{-3}$), respectively; α (cm^{-1}) and n (–) are fitting parameters of soil water characteristic curve; l (–) is the pore connectivity parameter (=0.5); and S_e (–) is the relative saturation. Marquardt–Levenberg type parameter estimation algorithm is implemented in HYDRUS-1D for inverse estimation of these soil hydraulic parameters.

For the simulation of soil water movement in paddy plots, 1 m deep paddy soil domain was represented the soil columns of experimental paddy plots since the groundwater depth was always lower than 1 m. Moreover, Garg et al. (2009) used the 80 cm soil depth domain and obtained the reasonable simulation results. For the objectivity of evaluating the water balances of lowland paddy fields with extremely shallow groundwater, the selected soil domain of 1 m deep is enough to find the groundwater capillary rise. The initial soil water condition of the soil domain was the soil water content, calculated from measured water pressure head based on van Genuchten's $\theta-h$ relationship, at the day before transplanting. The lower boundary condition was the measured daily pressure head derived from the water table depth, and the upper boundary condition was the atmospheric boundary condition with ponded water. This atmospheric boundary condition consisted of rainfall, evapotranspiration and irrigation. In that irrigation was assumed to be uniform rainfall. The left and right side boundaries of soil domain were treated as no-flux boundaries, as the plastic sheet greatly prevent lateral soil water flow between paddy plots and we expected minimal lateral seepage during the period of experiment.

The simulation was carried out in two steps: (i) forward simulation for each plot using measured soil hydraulic parameters which were listed in Table 2. (ii) Inverse estimation of the saturated hydraulic conductivity of PPL using measured pressure head and Marquardt–Levenberg type parameter estimation algorithm. In order to full use of the measured soil hydraulic parameters and decrease the uncertainties of parameter optimization, we just selected the saturated hydraulic conductivity of PPL for calibration, since PPL has extremely low saturated hydraulic conductivity and is mostly hard to measure accurately. Moreover, the PPL largely determines the soil preferential water flow in paddy fields (Sander and Gerke, 2007). Water pressure head values measured at 18, 33, and 72 cm soil depths were used as the auxiliary variable in the objective function. Hence, 48 set of time series data (3 depths, 8 plots, and 2 growing seasons) for piezometric and tensiometers heads were used to estimate saturated hydraulic conductivity of PPL. In this inverse modeling process, saturated hydraulic conductivity of PPL derived by the pressure head data in 2010 were used as input to predict the pressure head during 2011 and vice versa.

Two statistical procedures were used to assess the level of agreement between the simulated and observed data:

(i) Root mean square error (RMSE):

$$\text{RMSE} = \sqrt{\frac{\sum_{i=1}^n (P_i - O_i)^2}{n}} \quad (4)$$

(ii) Nash–Sutcliffe modeling efficiency (NSE) (Nash and Sutcliffe, 1970):

$$\text{NSE} = 1 - \frac{\sum_{i=1}^n (O_i - P_i)^2}{\sum_{i=1}^n (O_i - \bar{O})^2} \quad (5)$$

where P_i is the predicted pressure head corresponding to the observed pressure head O_i (cm), n is the number of data pairs, and \bar{O} is the observed average pressure head (cm).

3. Results and discussion

3.1. Soil properties and groundwater depth

Table 2 shows the mean values and variations for soil bulk density (ρ_b), texture properties and parameters of the water retention curves, as well as saturated hydraulic conductivities (K_s) measured from different soil layers in experimental paddy plots by laboratory analysis of core samples. The physical analysis indicated that PPL had the highest ρ_b with a range of 1.52 – 1.60 g cm^{-3} , and lowest K_s with a range of 0.26 – 0.70 cm d^{-1} , which was about only 6.5% of that of CHL and 2.6% of that of IHL. Soils above and below PPL were generally less compact. This is a common feature with the puddled paddy soil profiles as the puddling operation promotes illuviation of finer soil fractions to form a compacted layer (Tournebize et al., 2006; Bouman et al., 2007b; Garg et al., 2009). The measured K_s (0.48 cm d^{-1}) of PPL is much higher than what Wopereis et al. (1994) (0.036 cm d^{-1}) and Chen and Liu (2002) (0.05 cm d^{-1}) measured at specific paddy fields. However, it is lower than what Garg et al. (2009) (1.3 cm d^{-1}) measured. **Table 2** also suggests that soils of PPL and CHL have large variability of K_s , which shows the difficulty to simulate soil water flow with unique K_s and the necessity to calibrate it.

Analyzing the measured groundwater depth, we found that the difference of measured groundwater depth between all plots was extremely small as plots were next to each other and the area of experimental paddy fields is small. Therefore, we ignored the difference of groundwater depth between AWD plots and CFL plots for bottom boundary setting up for both forward simulation and inverse modeling. The average groundwater depth during the rice growing season was shown in Fig. 2. The groundwater depth ranged from 66.4 to 93.6 cm. It was slightly deeper than other reported experiments (about 40 cm) (Belder, 2004; Cabangon et al., 2004; Peng et al., 2011). Generally, groundwater of paddy fields in 2010 was deeper than that in 2011 because of the relative less rainfall input in 2010. The water table did not always fluctuate with the rainfall and irrigation, because sometimes it was controlled by the water level in drainage ditch that passes through the experimental paddy fields (Fig. 1).

3.2. Grain yield and water productivity

Water productivity (kg grain m^{-3} water) was calculated as grain yields divided by total water input that includes rainfall and irrigation. Grain yields ranged from 6044 to 7864 kg ha^{-1} , while water productivity from 0.80 to $1.24 \text{ kg grain m}^{-3}$ water input (Table 5). Although the AWD practice decreased grain yields, on average, by 9.6%, it increased water productivity by 32.2% in two experimental years, compared to CFL practice. These results were slightly different from our previous experimental results that showed there were no significant grain yield variations with AWD

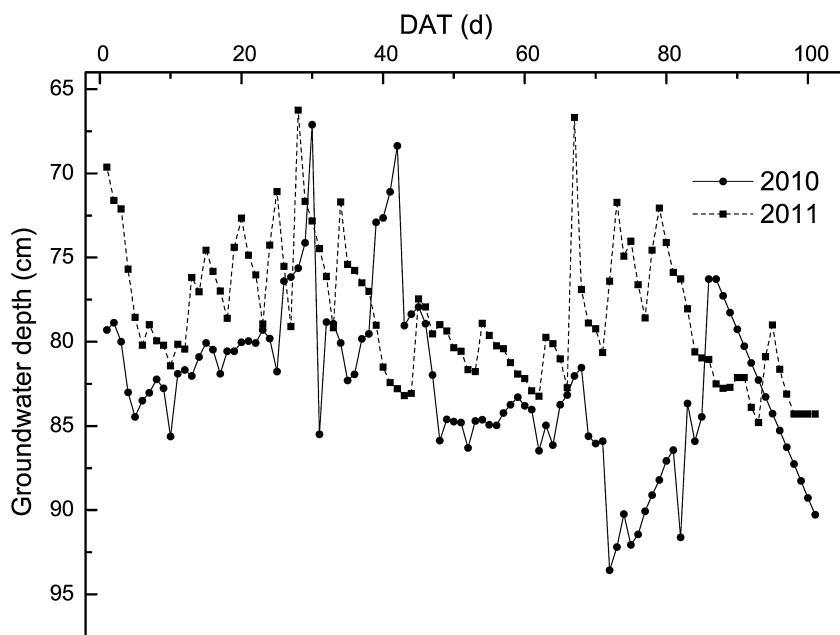


Fig. 2. Groundwater table of experimental paddy field in 2010 and 2011.

practice compared with CFI practice (Tan et al., 2013). This was caused by the deep groundwater as depth of water table was 15–40 cm (Tan et al., 2013) in previous experiment while 66–94 cm in this experiment (Fig. 2). It indicates that relatively shallow water table is of great importance to the success of the AWD practice without affecting the crop yield, which was also found by Belder et al. (2005).

3.3. Simulation of soil water regime

Because of little water input to AWD plots during the last few days ($DAT = 80\text{--}103$) in 2011 (Fig. 3), the pressure head of soil depth of 18 cm amounted almost -2000 cm as simulated, which extremely lower than usual pressure head and cannot be accurately measured by our tensiometers. In order to eliminate the huge effect of these extremely low values on the statistics of model performance, we neglected the pressure head values of these last seven days for modeling and statistical analysis.

Using the measured values of hydraulic parameters of each paddy plot (Table 2), the water movement during the rice growing season was simulated respectively. By comparing measured and simulated pressure heads of soil depth of 18, 33 and 72 cm, Table 3 shows the statistics of agreement. The model performance for CFI plots was better than that for AWD plots as the RMSE of AWD plot was averagely 1.16 times of that of CFI plots, and NSE of AWD plot was 9.6% lower than that of CFI plots on average. This difference is also reflected by other modeling results, such as that done by Garg

et al. (2009) and Sander and Gerke (2009). Thus, the point estimated soil hydraulic properties did not represent the plot due to landscape heterogeneity and preferential flow. The RMSE of pressure head ranged 1.80–9.43 cm with the mean of 5.17 cm, and the NSE ranged 0.56–0.94 with the mean of 0.80, which was largely lower than that of simulations Wang et al. (2010) conducted using HYDRUS-1D. The worst goodness-of-fit between measured and simulated pressure data occurred at soil depth of 33 cm in AWD plots.

As the measured pressure head values of Plot 2 (AWD) and Plot 6 (CFI) closest approach to the respective mean values of all four plots, the measured and simulated pressure head in 18, 33 and 72 cm at Plot 2 and Plot 6 was selected to show in Fig. 3. Comparison of these two pressure head processes indicate that the high pressure head occurred during the ponded days was always underestimated, while the extremely low pressure head in drying days was usually overestimated at soil depth of 18 cm in AWD plots both in 2010 and 2011. In CFI plots, the positive pressure head at soil depth of 18 cm was usually overestimated before the rice growth stage of late tillering ($DAT = 1\text{--}30$). In that time, the decrease of measured pressure head sometimes was not found by forward simulation. Therefore, it is motivated to conduct inverse modeling for water balance analysis.

Calibrated by the 48 sets of pressure head time series data, we estimated the respective saturated hydraulic conductivity of paddy plots. Fig. 3 shows simulated pressure values from inverse modeling for soil depth of 18, 33 and 72 cm and Table 3 shows the model performance of inverse modeling. The optimized K_s

Table 3
Model performance statistics for predicted pressure head in experimental AWD and CFI paddy plots.

Year	Treatment	Pressure head			
		RMSE ^a (cm)	RMSE ^b (cm)	NSE ^a	NSE ^b
2010	AWD	6.82 ± 1.62^c	2.22 ± 0.43	0.80 ± 0.06	0.95 ± 0.02
	CFI	3.42 ± 1.18	1.56 ± 0.62	0.86 ± 0.08	0.96 ± 0.02
2011	AWD	7.32 ± 2.11	2.15 ± 0.53	0.72 ± 0.16	0.96 ± 0.02
	CFI	3.13 ± 1.33	1.73 ± 0.77	0.82 ± 0.08	0.95 ± 0.01

^a Model performance from forward simulation with measured mean saturated hydraulic conductivity.

^b Calibrated performance from inverse modeling with the optimized saturated hydraulic conductivity.

^c Values after the plus/minus is the standard deviation of four replicate plots.

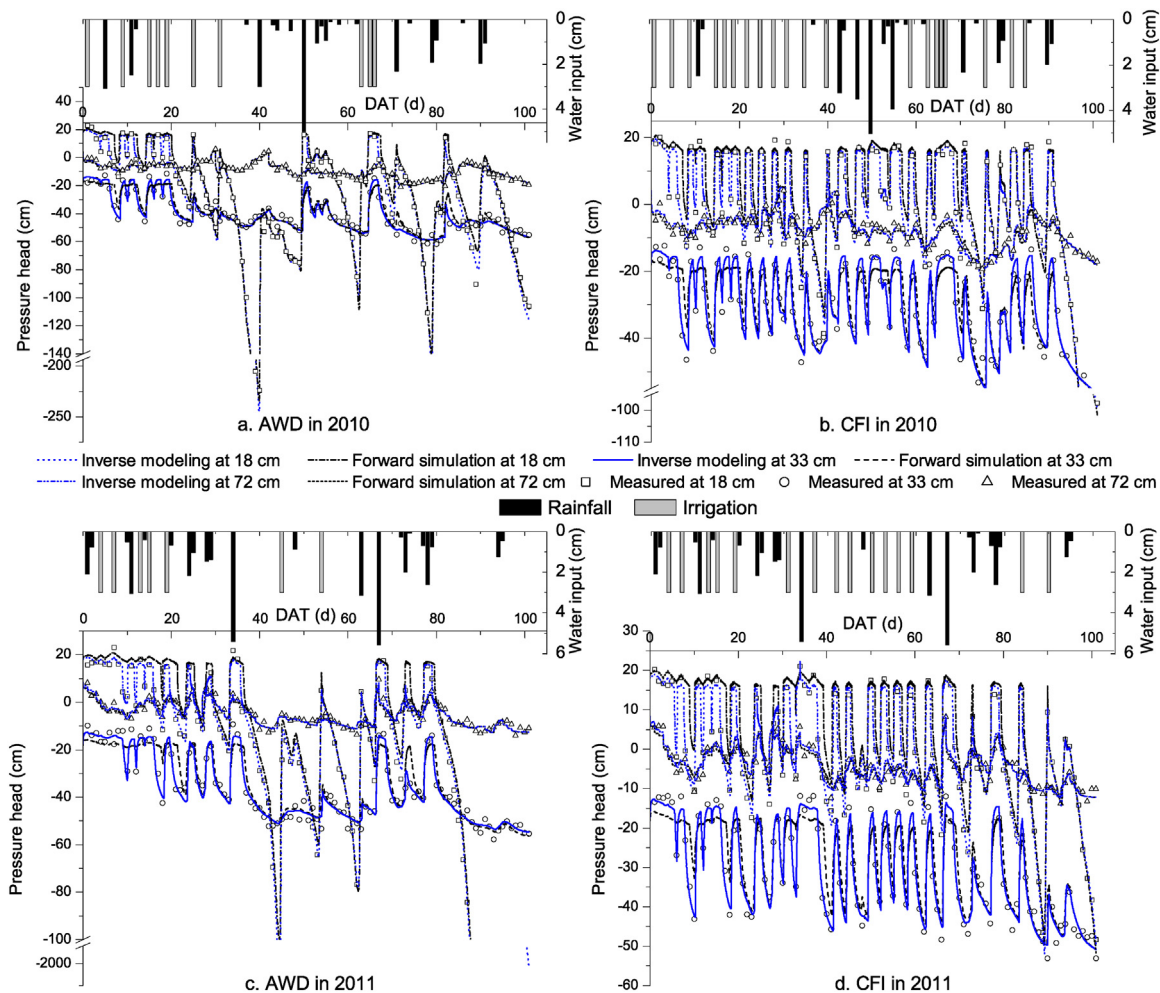


Fig. 3. Measured, forward simulated and inverse modeling pressure head at the soil depth of 18, 33 and 72 cm in paddy fields under AWD (Plot 2) and CFI (Plot 6) during the rice growing season of 2010 and 2011.

values of PPL were 0.66, 0.68, 0.69 and 0.69 cm d⁻¹ for AWD plots (mean of 0.68 cm d⁻¹), and 0.53, 0.53, 0.54, and 0.55 cm d⁻¹ for CFI plots (mean of 0.54 cm d⁻¹). The simulated pressure head processes from inverse modeling (Fig. 3) both in 2010 and 2011 were greatly improved through inverse modeling of K_s values, compared to that of forward simulation. This improvement was especially evident at soil depth of 18 and 33 cm. The RMSEs decreased 59.3% and NSE increased 19.9% on average by inverse modeling, compared to the former forward simulation. Although Garg et al. (2009) and Sander and Gerke (2009) suggested to use dual-porosity model for capturing the characteristics of pressure head in paddy field with preferential flow, from our inverse modeling of saturated hydraulic conductivity of PPL, the single-porosity model included in HYDRUS-1D can properly simulate the water flow in multi-layer paddy soil flow where the PPL plays an important role in determining the vertical pressure head distribution. The average NSE reached 0.93–0.98, which indicates that the simulation results from inverse modeling are reasonable for water balance analysis.

The difference of calibrated saturated hydraulic conductivity between AWD and CFI plots may be associated with the impact of AWD on the increasing of preferential soil flow in lowland paddy fields. The occurrence and disappear of cracks with different susceptibilities to swelling and shrinkage caused dynamical change of hydraulic conditions in paddy fields as a results of AWD (Garg et al., 2009; Sander and Gerke, 2007). However, as the landscape heterogeneity may also cause vary soil hydraulic properties between

experimental paddy plots, and there was no enough evidence for preferential flow in experimental paddy fields, the relationship between calibrated saturated hydraulic conductivity and preferential flow caused by AWD practice cannot be addressed in this study.

3.4. Pressure distribution and water balance

The statistical values of measured pressure were shown in Table 4. During paddy experiments in both 2010 and 2011, pressure head at 18, 33 and 72 cm soil depths fluctuated depending on the water input (Fig. 3). There were great variations in AWD and CFI plots with respect to pressure head distribution and temporal change pattern. The pressure head generally changed with the rainfall and irrigation. When rainfall and irrigation flooded paddy fields, the pressure head increased, although the amplitude of variation decreased from top to bottom in soil profile. The pressure head in the CHL was most sensitive with the rainfall and irrigation, since these water inputs were firstly perched at CHL by PPL and then slowly infiltrated downward to bottom soil or was lost by evapotranspiration.

Generally, the pressure head of all paddy fields soil was negative, showed by the mean value of all three measured soil depth, which means that soil were unsaturated during the rice growing season both in CFI and AWD plots. The pressure head of AWD plots varied greatly compared to that of CFI plots both in 2010 and 2011,

Table 4

Statistics of measured pressure head in experimental AWD and CFI paddy plots.

Year	Treatment	Soil depth (cm)	Mean (cm)	Standard deviation (cm)	Minimum (cm)	Maximum (cm)
2010	AWD	18	-31.8 ± 8.3 ^a	44.8 ± 10.2	-223.9 ± 46.3	22.7 ± 2.8
		33	-40.7 ± 2.8	12.5 ± 2.1	-61.7 ± 12.3	-11.6 ± 3.8
		72	-9.3 ± 1.3	5.6 ± 1.7	-21.0 ± 2.4	6.0 ± 1.1
	CFI	18	-3.8 ± 1.6	22.7 ± 2.4	-97.8 ± 8.7	20.1 ± 0.8
		33	-31.3 ± 4.2	12.9 ± 3.7	-64.7 ± 17.6	-12.3 ± 3.9
		72	-8.1 ± 0.6	4.9 ± 0.9	-19.3 ± 2.2	4.3 ± 0.7
2011	AWD	18	-86.1 ± 20.8	219.8 ± 48.7	-968.0 ± 82.9	23.0 ± 2.4
		33	-36.5 ± 3.7	14.4 ± 3.3	-57.9 ± 11.6	-9.3 ± 2.2
		72	-5.0 ± 0.4	5.2 ± 1.4	-14.1 ± 1.4	9.6 ± 1.3
	CFI	18	-2.0 ± 1.8	15.2 ± 1.2	-48.4 ± 6.8	21.1 ± 0.6
		33	-30.9 ± 12.4	12.6 ± 4.8	-53.1 ± 19.7	-11.8 ± 2.5
		72	-4.6 ± 0.6	4.9 ± 0.9	-13.8 ± 0.9	8.2 ± 1.1

^a Values after the plus/minus is the standard deviation of four replicate plots.

especially at soil depth of 18 cm. Owing to the timely irrigation, the pressure in the 18 cm of CFI paddy plots was always larger than -25 cm in rice growing season except the last 10 naturally drainage days. The range of pressure head at soil depth of 18 cm in AWD plots was significantly larger than that in CFI plots, shown by the minimum and maximum pressure head in Table 4. The AWD practice just significantly affected the pressure head in soil depth of 18 cm, so it is important to observe the top soil pressure head for AWD irrigation in paddy fields. There were greater variations of measured pressure head in four AWD plots at soil depth of 18 cm, compared to that of 33 and 72 cm, while there were greater variations of measured pressure head in four CFI plots at soil depth of 33 cm, compared to that of 18 and 72 cm. This was the coupled effect of hydraulic properties of soil layers and soil water flow directions (capillary rise or downward percolation). Because of less water input to AWD plots after growth stage of late tillering (DAT = 25–30) in 2011, the mean pressure head at soil depth of 18 cm was lower than that in 2010. However, the mean pressure head at soil depth of 33 and 70 cm in 2011 was almost the same as that in 2010, owing to the contribution of shallow water table and groundwater capillary rise.

The soil in depth of 72 cm was almost saturated both in AWD and CFI paddy plots as it approached to the water table. Garg et al. (2009) reported that the pressure head of soil depth of 60 cm reached 60 cm because of the extremely low water table and the low saturated hydraulic conductivity (1.2 cm d^{-1}) of plow pan soil in their experimental fields. However, Tournebize et al. (2006) measured and simulated the pressure head in soil depth of 85 cm and showed that it ranged from -75 to -200 cm, simply because of the deep water table and the high saturated hydraulic conductivity (13.2 cm d^{-1}) of plow pan. In their modeling simulation, the bottom boundary of paddy fields was regarded as free drainage boundary. Thus, the water table in paddy fields and saturated hydraulic conductivity of plow pan is significant for pressure head distribution in soil profiles.

Fig. 4 shows the changes of vertical simulated pressure head distribution in Plot 2 which was induced by large (5.02 cm) rainfall in DAT = 50. Usually, the soil below 60 cm was nearly saturated and varied little during the rice growing season, which was different from the result of Tournebize et al. (2006), since groundwater depths in their experimental fields were extremely deep. The rainfall and irrigation did not significantly affect pressure head in IHL. The pressure head of CHL and PPL increased significantly with different degrees from DAT = 49–50. After rainfall at DAT = 50, the vertical pressure distribution typically reflected the importance of PPL for soil water regime in flooded paddy fields, where perched water formed above the PPL while soil under or in the PPL was unsaturated. Our measured and simulated pressure head distribution and soil water regime were similar to what Ye (1991)

calculated based on the analytical equation for structured paddy multi-layer soil with PPL. The two turning points existed near the interface of soil layers, which indicates that identification of the thickness and location of plow pan is important for paddy soil water flow analysis.

From the inverse modeling simulation, Fig. 5 shows bottom flux at soil depth of 1 m in paddy fields under AWD (Plot 2) and CFI (Plot 6), in which the negative value represents the percolation while the positive value illustrates the groundwater capillary rise. Groundwater moved upward by capillarity and transpiration suction during the dry days, mostly happened at the rice growth stage of late tillering, booting and heading. Because of the high water table at DAT = 15–35 in 2011 (Fig. 2), the daily groundwater capillary rise was higher than that in 2010 at both AWD and CFI plots, although the surface soil pressure head of two years were similar (Fig. 3). However, the number of days that existed groundwater capillary rise in this period of 2010 was more than that in 2011 due to the dry soil water regime in fields. Also, the daily groundwater capillary rise in AWD plots was larger than that in CFI plots, which was more evident in 2010. The amount of days when groundwater flow happened in AWD plots (27 d) was twice more than that in CFI plots (12 d). The percolation variations between AWD and CFI plots were significant, especially during the DAT = 50–101, as the soil was controlled to be drier and have lower pressure gradient for percolation in AWD plots following experimental irrigation schedule.

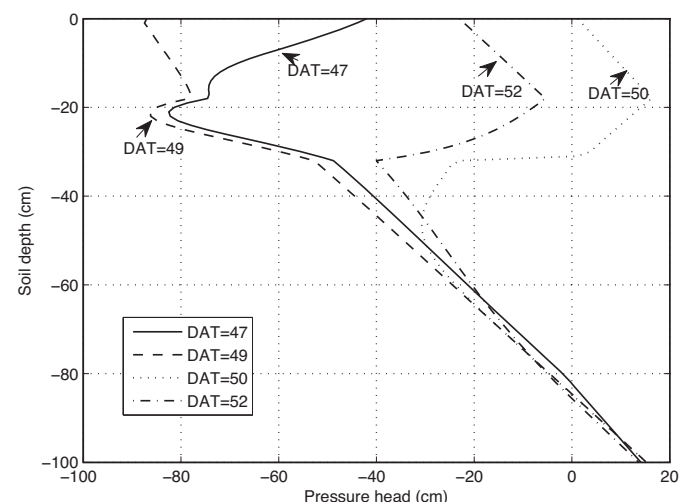


Fig. 4. Simulated vertical pressure head distribution variations in AWD (Plot 2) before and after heavy rainfall in DAT = 50 of 2010.

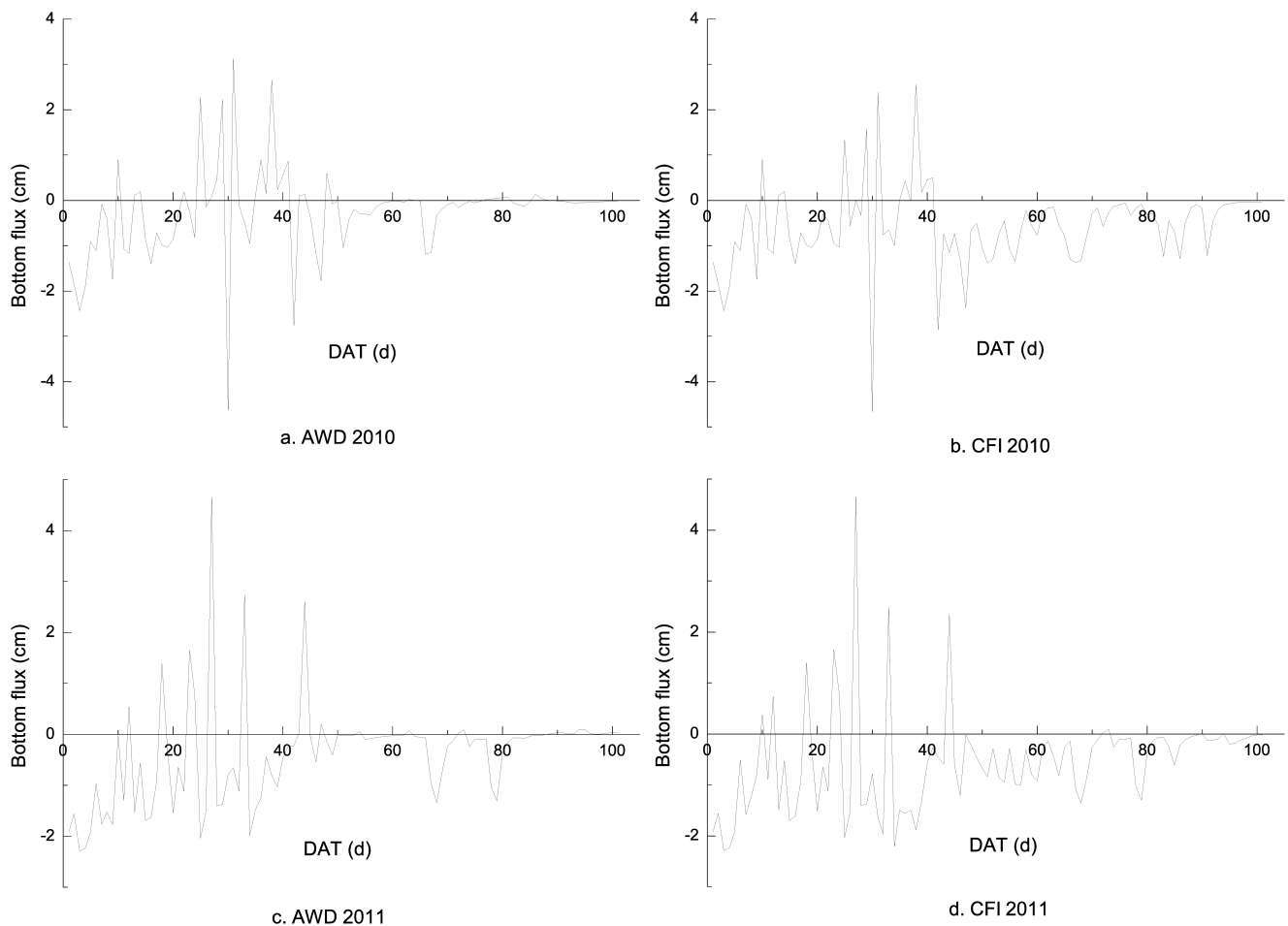


Fig. 5. Bottom water flux at soil depth of 1 m in paddy field under AWD (Plot 2) and CFI (Plot 6) during the rice growing season of 2010 and 2011. The negative value represents the percolation while the positive value illustrates the groundwater capillary rise.

Fig. 6 schematically shows the water balance components in the paddy plots. The water balances in paddy plots during the rice growing season were estimated based on the following equation:

$$\Delta SWS = R + I + GWR - ET - P \quad (6)$$

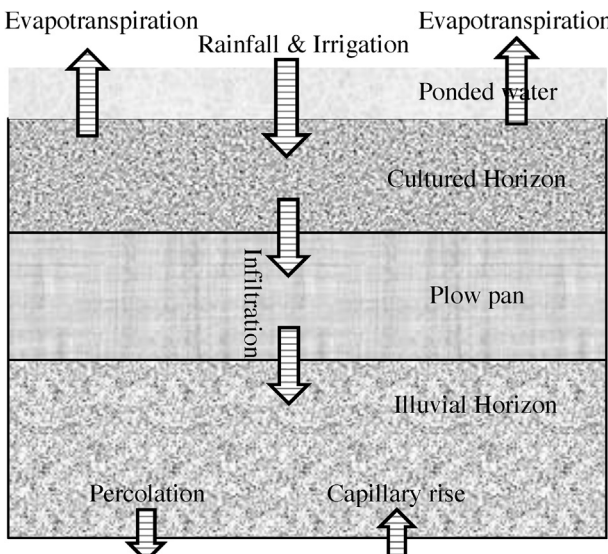


Fig. 6. Schematic diagram of water balance components in paddy fields.

where ΔSWS is the change of soil water storage from rice transplanting to harvesting (mm), which is the soil water consumption during the rice growing season. R and I is the measured rainfall and irrigation (mm), respectively. GWR is the groundwater capillary rise (mm), and P is the percolation (mm). The amount of these two components is the simulation results as above mentioned. ET is the evapotranspiration (mm), which was estimated by multiplying reference evapotranspiration derived from Penman–Monteith equation by the rice coefficient (Allen et al., 1998), based on meteorological data.

The water balances of paddy plots under AWD and CFI were shown in Table 5. Because paddy soil was almost saturated with ponded water before the rice transplanting and very dry at the day of harvest, we regarded the differences of soil water storage between before rice transplanting and after rice harvesting as soil water consumption. There was large difference between AWD and CFI paddy plots in terms of year and water balance components. Water inputs in AWD plots (597.4 mm in 2010 and 576.5 mm in 2011) were largely lower than that in CFI plots (897.4 mm in 2010 and 816.5 mm in 2011). Since the rainfall of 2010 was 38.4% lower than that of 2011, the irrigation volume of 2010 was 62.5% in AWD plots and 43.8% in CFI plots higher than that of 2011, respectively. The AWD plots saved 330 mm in 2010 and 240 mm irrigation water, compared to CFI plots.

The percolation of AWD plots was also 38.2–40.3% in 2010 and 23.3–27.2% in 2011 lower than that of CFI plots on average (Table 5). Note that the percolation losses (353–718 mm) were very large and usually even larger than the consumptive water use (ET). To

Table 5

Water balance components, grain yields and water productivity in paddy plots.

Year	Treatment (mm)	Irrigation ^a (mm)	Rainfall ^a (mm)	Evapotranspiration ^b (mm)	Groundwater capillary rise ^c (mm)	Percolation ^c (mm)	Soil water consumption (mm)	Grain yields ^a (kg ha ⁻¹)	Water productivity (kg grain m ⁻³ water input)
2010	AWD	390.0	207.4	412.1	162.6 ± 45.6 ^d	408.1 ± 55.2	60.2 ± 9.6	6849 ± 632	1.15 ± 0.09
	CFI	690.0	207.4	412.1	106.3 ± 29.4	674.5 ± 38.8	82.9 ± 9.4	7536 ± 328	0.84 ± 0.04
2011	AWD	240.0	336.5	335.3	152.1 ± 33.6	530.0 ± 39.1	136.8 ± 5.5	6628 ± 584	1.15 ± 0.09
	CFI	480.0	336.5	335.3	145.2 ± 12.4	695.7 ± 22.7	69.3 ± 10.3	7368 ± 405	0.90 ± 0.05

^a Measured values from in situ measurement.^b Calculated by multiplying reference evapotranspiration derived from Penman–Monteith equation by the rice coefficient (Allen et al., 1998), based on meteorological data.^c Derived from model simulation.^d Values after the plus/minus is the standard deviation of four replicate plots.

decrease this percolation, the designed irrigation schedule may be improved by increasing the critical soil matric potential for triggering irrigation, if the rice yields are not influenced significantly. These percolation losses were also larger than that of our previous measured (258–496 mm) in other paddy fields with heavier clay soil (Tan et al., 2013). The percolation can be reduced by increasing plowing to compact the soils of plow pan and decreases their hydraulic conductivities. Admittedly, the effectiveness of improving irrigation schedule and strengthening plowing on reducing percolation needs further investigations. However, the water use efficiency, defined as the ratio of the amount of evapotranspiration to that of water input, was 40.8–46.2% in CFI plots and 57.2–69.3% in AWD plots, and the daily percolation was 6.68–6.92 mm in CFI plots and 5.08–5.21 mm in AWD plots, which was within the range of reported values (Bouman and Tuong, 2001; Bouman et al., 2007b).

The groundwater capillary rise in 2010 varied greatly between AWD and CFI plots, while it was almost the same in 2011 in AWD and CFI plots. This was caused by the shallower groundwater depth and similar soil water regime of AWD and CFI plots in wet year of 2011. The amount of groundwater capillary rise was 26.1–27.4% in AWD plots, and 10.2–18.1% in CFI plots of amount of respective water input. The net percolation, which is equal to the percolation minus the groundwater capillary rise, per day was 2.3–3.8 mm d⁻¹ in AWD plots and 5.3–5.7 mm d⁻¹ in CFI plots. Thus, the increase of groundwater capillary rise and decrease of percolation contributed to the water saving in AWD plots, compared to CFI plots.

4. Conclusions

In order to better understand soil water regime in lowland paddy fields under AWD and CFI, field experiments were conducted to measure soil hydraulic properties and pressure head distribution. Model simulations with HYDRUS-1D were also carried out based on the measured pressure head distribution of soil profiles. The point measured soil hydraulic properties were not satisfied to describe the soil water flow in paddy fields. The inverse modeling indicated that measurement of soil pressure head distribution over a growing season could provide soil hydraulic parameters for predicting soil water regime in lowland paddy fields under AWD, coupled with the model simulation. Thus, it is helpful to specifically design irrigation schedule of AWD for lowland paddy fields with different soil properties.

This study also demonstrates that the designed irrigation schedule of CFI in our study was significantly over-irrigated, compared to that of AWD. Measurement and modeling results showed that the practice of AWD largely decreased the irrigation water compared to CFI. This was mostly due to the reduction of percolation and increase of groundwater capillary rise. The contribution of groundwater capillary rise for water saving irrigation should be considered in designing of irrigation schedule as the amount of groundwater capillary rise in AWD plots amounts to 26.1–27.4% of water input.

In lowland paddy fields, the shallow groundwater water table and dry environment of surface soil was helpful to upward movement of soil water and increasing the groundwater capillary rise.

Acknowledgments

The authors are grateful to Hua Zhang and Gang Pan for their excellent technical assistance during the field work. The study was financially supported by the National Key Technologies R&D Program of China during the 12th Five-year-Plan Period (No. 2012BAD08B05).

References

- Allen, R.G., Pereira, L.S., Raes, D., Smith, M., 1998. *Crop Evapotranspiration – Guidelines for Computing Crop Water Requirements*. FAO Irrigation and Drainage Paper 56. Food and Agriculture Organization (FAO) of the United Nations, Rome, Italy.
- Belder, P., 2004. Effect of water-saving irrigation on rice yield and water use in typical lowland conditions in Asia. *Agric. Water Manage.* 65 (3), 193–210.
- Belder, P., Spiertz, J., Bouman, B., Lu, G., Tuong, T., 2005. Nitrogen economy and water productivity of lowland rice under water-saving irrigation. *Field Crop Res.* 93 (2–3), 169–185.
- Belder, P., Bouman, B., Spiertz, J., 2007. Exploring options for water savings in lowland rice using a modelling approach. *Agric. Syst.* 92 (1–3), 91–114.
- Boling, A., Bouman, B., Tuong, T., Murty, M., Jatmiko, S., 2007. Modelling the effect of groundwater depth on yield-increasing interventions in rainfed lowland rice in Central Java, Indonesia. *Agric. Syst.* 92 (1–3), 115–139.
- Bouman, B.A.M., Feng, L., Tuong, T., Lu, G., Wang, H., Feng, Y., 2007a. Exploring options to grow rice using less water in northern China using a modelling approach II. Quantifying yield, water balance components, and water productivity. *Agric. Water Manage.* 88 (1–3), 23–33.
- Bouman, B.A.M., Humphreys, E., Tuong, T., Barker, R., 2007b. Rice and water. *Adv. Agron.* 92, 187–237.
- Bouman, B.A.M., Kropff, M.J., Tuong, T.P., Wopereis, M.C.S., ten Berge, H.F.M., van Laar, H.H., 2001. *ORYZA2000: Modelling Lowland Rice*. International Rice Research Institute, Wageningen University and Research Centre, Los Banos, Philippines, Wageningen, Netherlands, pp. 235.
- Bouman, B.A.M., Tuong, T.P., 2001. Field water management to save water and increase its productivity in irrigated lowland rice. *Agric. Water Manage.* 49, 11–30.
- Cabangon, R.J., Tuong, T.P., Castillo, E.G., Bao, L.X., Lu, G., Wang, G., Cui, Y., Bouman, B.A.M., Li, Y., Chen, C., Wang, J., 2004. Effect of irrigation method and N-fertilizer management on rice yield, water productivity and nutrient-use efficiencies in typical lowland rice conditions in China. *Paddy Water Environ.* 2 (4), 195–206.
- Chen, S.-K., Liu, C.W., 2002. Analysis of water movement in paddy rice fields (I) experimental studies. *J. Hydrol.* 260, 206–215.
- Chen, S.-K., Liu, C.W., Huang, H.-C., 2002. Analysis of water movement in paddy rice fields (II) simulation studies. *J. Hydrol.* 268, 259–271.
- Garg, K.K., Das, B.S., Safeeq, M., Bhadoria, P.B.S., 2009. Measurement and modeling of soil water regime in a lowland paddy field showing preferential transport. *Agric. Water Manage.* 96 (12), 1705–1714.
- Inthavong, T., Tsubo, M., Fukai, S., 2011. A water balance model for characterization of length of growing period and water stress development for rainfed lowland rice. *Field Crop Res.* 121 (2), 291–301.
- Janssen, M., Lennartz, B., 2009. Water losses through paddy bunds: methods, experimental data, and simulation studies. *J. Hydrol.* 369 (1–2), 142–153.
- Khepar, S.D., Yadav, A.K., Sondhi, S.K., Siag, M., 2000. Water balance model for paddy fields under intermittent irrigation practices. *Irrigation Sci.* 19, 199–208.
- Kukal, S.S., Hira, G.S., Sidhu, A.S., 2005. Soil matric potential-based irrigation scheduling to rice (*Oryza sativa*). *Irrigation Sci.* 23 (4), 153–159.

- Li, Y.H., 2001. Research and practice of water-saving irrigation for rice in China. In: Barker, R., Loeve, R., Li, Y., Tuong, T.P. (Eds.), Proceedings of an International Workshop on Water-Saving Irrigation for Rice, 23–25 March. Wuhan, China, pp. 135–144.
- Li, Y., Barker, R., 2004. Increasing water productivity for paddy irrigation in China. *Paddy Water Environ.* 2, 187–193.
- Liu, C.-W., Tan, C.-H., Huang, C.-C., 2005. Determination of the magnitudes and values for groundwater recharge from Taiwan's paddy field. *Paddy Water Environ.* 3 (2), 121–126.
- Loeve, R., Dong, B., Hong, L., Chen, C.D., Zhang, S., Barker, R., 2007. Transferring water from irrigation to higher valued uses: a case study of the Zhanghe irrigation system in China. *Paddy Water Environ.* 5 (4), 263–269.
- Luo, Y., Khan, S., Cui, Y., Peng, S., 2009. Application of system dynamics approach for time varying water balance in aerobic paddy fields. *Paddy Water Environ.* 7 (1), 1–9.
- Mao, Z., 2001. Water Efficient Irrigation and Environmentally Sustainable Irrigated Rice Production in China. International Commission on Irrigation and Drainage, <http://www.icid.org/wat.mao.pdf>
- Mishra, H., Rathore, T., Pant, R., 1990. Effect of intermittent irrigation on groundwater table contribution, irrigation requirement and yield of rice in Mollisols of the Tarai region. *Agric. Water Manage.* 18 (3), 231–241.
- Nash, J.E., Sutcliffe, J.V., 1970. River flow forecasting through conceptual models. Part I. A discussion of principles. *J. Hydrol.* 10 (3), 282–290.
- Peng, S.Z., Yang, S.H., Xu, J.Z., Luo, Y.F., Hou, H.J., 2011. Nitrogen and phosphorus leaching losses from paddy fields with different water and nitrogen managements. *Paddy Water Environ.* 9 (3), 333–342.
- Peters, A., Durner, W., 2008. Simplified evaporation method for determining soil hydraulic properties. *J. Hydrol.* 356 (1–2), 147–162.
- Sander, T., Gerke, H.H., 2007. Preferential flow patterns in paddy fields using a dye tracer. *Vadose Zone J.* 6 (1), 105–115.
- Sander, T., Gerke, H., 2009. Modelling field-data of preferential flow in paddy soil induced by earthworm burrows. *J. Contam. Hydrol.* 104 (1–4), 126–136.
- Simunek, J., Sejna, M., van Genuchten, M.Th., 1998. The HYDRUS-1D Software Package for Simulating the One-dimensional Movement of Water, Heat, and Multiple Solutes in Variably-saturated Media. Version 2.0, IGWMC-TPS-70. International Ground Water Modeling Center, Colorado School of Mines, Golden Colorado, pp. 202.
- Tan, X., Shao, D., Liu, H., Yang, F., Xiao, C., Yang, H., 2013. Effects of alternate wetting and drying irrigation on percolation and nitrogen leaching in paddy fields. *Paddy Water Environ.* 11, 381–395.
- ten Berge, H.F.M., Metselaar, K., Jansen, M.J.W., Agustin, E.M. d.S., Woodhead, T., 1995. The SAWAH rice land hydrology model. *Water Resour. Res.* 31 (11), 2721–2732.
- Tournebize, J., Watanabe, H., Takagi, K., Nishimura, T., 2006. The development of a coupled model (PCPF-SWMS) to simulate water flow and pollutant transport in Japanese paddy fields. *Paddy Water Environ.* 4 (1), 39–51.
- Tuong, T.P., Bouman, B.A.M., Mortimer, M., 2005. More rice, less water-integrated approaches for increasing water productivity in irrigated rice-based systems in Asia. *Plant Prod. Sci.* 8 (3), 231–241.
- van Genuchten, M., 1980. A closed-form equation for predicting the hydraulic conductivity of unsaturated soils. *Soil Sci. Soc. Am. J.* 44 (5), 892–898.
- Wang, H., Ju, X., Wei, Y., Li, B., Zhao, L., Hu, K., 2010. Simulation of bromide and nitrate leaching under heavy rainfall and high-intensity irrigation rates in North China Plain. *Agric. Water Manage.* 97 (10), 1646–1654.
- Wopereis, M.C.S., Bouman, B.A.M., Kropff, M.J., ten Berge, H.F.M., Maligaya, A.R., 1994. Water use efficiency of flooded rice fields I. Validation of the soil–water balance model SAWAH. *Agric. Water Manage.* 26 (4), 277–289.
- Ye, Z., 1991. Pressure distribution on the vertical profile in paddy field and steady specific discharge of water through the profile during flood irrigation. *J. Hydraul. Eng.* 2, 1–10 (in Chinese).
- Zhang, H., Xue, Y., Wang, Z., Yang, J., Zhang, J., 2009. An alternate wetting and moderate soil drying regime improves root and shoot growth in rice. *Crop Sci.* 49 (6), 2246.